DALTON
FULL PAPER

# Copper(II) complexation by human and mouse fragments (11–16) of β-amyloid peptide

**Teresa Kowalik-Jankowska,*[a] Monika Ruta-Dolejsz,[a] Kornelia Wiśniewska,[b] Leszek Łankiewicz[b] and Henryk Kozłowski[a]**

[a] *Faculty of Chemistry, University of Wrocław, F. Joliot-Curie 14, 50-383 Wrocław, Poland. Fax: (048)(71)328 23 48; E-mail: TerKow@Wchuwr.Chem.Uni.Wroc.pl*
[b] *Faculty of Chemistry, University of Gdańsk, Sobieskiego 18, 80-952 Gdańsk, Poland*

***Received 28th July 2000, Accepted 30th October 2000***
***First published as an Advance Article on the web 1st December 2000***

A potentiometric and spectroscopic (UV-Vis, CD, NMR and EPR) study of copper(II) bonding to the N-terminal (11–16) of human and mouse fragments of β-amyloid peptide (EVHHQK-$NH_2$, EVRHQK-$NH_2$ and their N-blocked derivatives) was performed. The results indicate that the hexapeptide amide EVHHQK-$NH_2$ forms in the pH range 4.5–10.5 complexes in which the coordination of copper(II) is typical {$NH_2$, $2N^-$, $N_{Im}$} for the peptide sequence Xaa-Yaa-His. The mouse fragment containing the N-terminal amino group free in a wide pH range is coordinated through the terminal amino group, carbonyl oxygen or one or two deprotonated amide nitrogens from the N-termini, while the fourth coordination site is occupied by a nitrogen donor of imidazole in the form of a macrochelate. When the amino group is blocked (Ac-EVRHQK-$NH_2$) the imidazole nitrogen of the histidine residue acts as an anchoring bonding site and at higher pH the 3N and 4N complexes are formed with the amide nitrogens coordinated. A blocked hexapeptide modeling a part of human β-amyloid peptide (Ac-EVHHQK-$NH_2$) forms complexes with coordination through imidazole nitrogens both of histidine residues over a broad pH range. With increasing pH the amide nitrogens are also coordinated. In a wide pH range including physiological, Ac-EVHHQK-$NH_2$ (human fragment) is much more effective in copper(II) ion bonding than is Ac-EVRHQK-$NH_2$ (mouse fragment).

## 1 Introduction

Alzheimer's disease (AD) is the most common form of dementia in the elderly.[1] The major neuropathological hallmarks of the disorder are abnormal accumulations of intracellular neurofibrillary tangles and extracellular amyloid plaques in vulnerable brain regions.[2] The major component of senile plaques is the β amyloid peptide (Aβ),[3] a 39–43 amino acid long peptide, deriving from the amyloid precursor protein (APP).[4] Cleavage of APP by unidentified proteases, referred to as β- and γ-secretases,[5–7] generates the β-amyloid peptide.

The rats and mice Aβ region contains three amino acid substitutions (R5G; Y10F; H13R) as compared to human Aβ.[8,9] These changes have been shown to alter the structure and properties of the Aβ peptides[10–12] as well as the processing of APP. Under similar cellular conditions, processing of rodent APP gives substantially reduced levels of Aβ as compared to human APP.[13] These sequence alternations might therefore be responsible for the virtual absence of Aβ deposits in normal or aged rodent brain.[12,14]

The studies indicate that APP expression specifically modulates copper homeostasis in the liver and cerebral cortex, the latter being a region of the brain particularly involved in AD.[15] The perturbations to APP metabolism could initiate pathological changes associated with copper metabolism. Decreased APP could raise copper levels in the cerebral cortex which in turn promotes human Aβ aggregation[16] as well as increased free radical production from Aβ and/or cell-associated APP.[17–19] The copper levels are abnormally elevated in amyloid where the concentration of copper has been measured at 30 μg $g^{-1}$ (≈0.5 mM, dry weight).[20] Extraction of copper may be the basis of the recent discovery that copper-selective chelators, such as bathocuproine, facilitate solubilization of Aβ from deposits in post-mortem AD brain specimens.[21] Therefore, these studies may suggest an important role for copper in AD pathogenesis.[22]

The present paper reports the results of combined spectroscopic and potentiometric studies on the copper(II) complexes of human and mouse β-amyloid peptide fragments (11–16). The peptides involved in the study are the human fragment (11–16H), Glu-Val-His-His-Gln-Lys-$NH_2$, EVHHQK-$NH_2$ and the mouse fragment (11–16M), Glu-Val-Arg-His-Gln-Lys-$NH_2$, EVRHQK-$NH_2$. To make the peptide a more relevant model, the N-terminal was blocked by acetylation and the human and mouse fragments Ac-Glu-Val-His-His-Gln-Lys-$NH_2$, Ac-EVHHQK-$NH_2$ (Ac-11–16H) and Ac-Glu-Val-Arg-His-Gln-Lys-$NH_2$, Ac-EVRHQK-$NH_2$ (Ac-11–16M), were also studied. This study was performed in order to examine the difference of the binding ability between the human and mouse fragments, especially the effect of the His-His sequence in a human fragment, on the formation of complexes with $Cu^{2+}$ ions.

## 2 Experimental

### 2.1 Peptide synthesis

Fragments of human (H) and mouse (M) β-amyloid peptide (βA4), Glu-Val-His-His-Gln-Lys-$NH_2$ (11–16H), Glu-Val-Arg-His-Gln-Lys-$NH_2$ (11–16M), Ac-Glu-Val-His-His-Gln-Lys-$NH_2$ (Ac-11–16H) and Ac-Glu-Val-Arg-His-Gln-Lys-$NH_2$ (Ac-11–16M), were obtained by a solid-phase method using Fmoc (Fmoc = 9-fluorenylmethoxycarbonyl) strategy with continuous-flow methodology (9050 Plus Millipore Peptide Synthesizer) on a polystyrene/polyethylene glycol graft copolymer resin (TentaGel R RAM Resin).[23] Attachment of the first amino acid to the resin and the next coupling steps were realised using diisopropylcarbodiimide (DIPCI) as a coupling reagent in the presence of 1-hydroxybenzotriazole (HOBt) in dimethylformamide (DMF)–*N*-methylpyrrolidone (NMP)–methylene chloride–Triton X-100 (33 : 33 : 33 : 1, v/v). Removal

of Fmoc protections during peptide synthesis was achieved by action of 20% piperidine solution in DMF–NMP (1:1, v/v) with addition of 1% Triton X-100.[24] In the case of peptides Ac-11–16H and Ac-11–16M the N-terminal amino group was acetylated using 1 M acetylimidazole in DMF.[24,25] All peptides were cleaved from the resin and deprotected using reagent B (88% trifluoroacetic acid, 5% phenol, 2% triisopropylsilane, 5% water) for 2 h at room temperature.[24]

The resulting crude peptides 11–16H, 11–16M, Ac-11–16H and Ac-11–16M were purified by reversed-phase high-performance liquid chromatography (RP-HPLC) using a $C_8$ Kromasil column (25 × 250 mm, 7 μm) and a linear gradient of 0–80% acetonitrile in 0.1% aqueous trifluoroacetic acid as a mobile phase. Their purity was assessed by RP-HPLC using a $C_8$ Kromasil column (4.6 × 250 mm, 5 μm) and a linear gradient of 0–80% acetonitrile in 0.1% aqueous trifluoroacetic acid as a mobile phase during 60 min and fast atom bombardment mass spectrometry (FAB-MS). Analytical data were as follows: 11–16H $R_t$(HPLC) = 12.33 min, *m/z* [$M^+$ + 1(FAB-MS)] = 775; 11–16M $R_t$(HPLC) = 12.95 min, *m/z* [$M^+$ + 1(FAB-MS)] = 796; Ac-11–16H $R_t$(HPLC) = 14.66 min, *m/z* [$M^+$ + 1(FAB-MS)] = 817; Ac-11–16M $R_t$(HPLC) = 14.86 min, *m/z* [$M^+$ + 1(FAB-MS)] = 838.

### 2.2 Potentiometric measurements

Stability constants for proton and $Cu^{2+}$ complexes were calculated from pH-metric titrations carried out in an argon atmosphere at 298 K using a total volume of 1.5 $cm^3$. Alkali was added from a 0.250 $cm^3$ micrometer syringe calibrated by both weight titration and the titration of standard materials. Ligand concentration $2 \times 10^{-3}$ mol $dm^{-3}$; metal-to-ligand ratio 1:1.1; ionic strength 0.1 mol $dm^{-3}$ ($KNO_3$); pH-metric titration on a MOLSPIN pH-meter system using a Russel CMAW 711 semi-micro combined electrode, calibrated in concentration using $HNO_3$,[26] number of titrations 2; method of calculation SUPERQUAD.[27] The samples were titrated in the pH region 2.5–10.5. Standard deviations ($\sigma$ values) quoted were computed by SUPERQUAD and refer to random errors only. They are, however, a good indication of the importance of the particular species involved in the equilibria.

### 2.3 Spectroscopic measurements

Solutions were of similar concentrations to those used in potentiometric studies. The $^1H$ NMR spectra were recorded on a Bruker Avance spectrometer at 500 MHz in $^2H_2O$ using TSP (sodium-2,2,3,3-tetradeuterio-3-trimethylsilylpropionate) as internal standard, ligand concentration 0.002 M and metal to ligand molar ratios 1:100 and 1:50. Spin–lattice relaxation rates were measured with inversion recovery pulse sequences and calculated by exponential regression analysis of the recovery curves of longitudinal magnetization components. EPR spectra were recorded on a Bruker ESP 300E spectrometer at X-band frequency (9.3 GHz) at 120 K. The parameters were calculated for spectra obtained at the maximum concentration of the particular species for which well resolved components were observed. Absorption spectra were recorded on a Beckman DU 650 spectrophotometer. Circular dichroism (CD) spectra were obtained on a JASCO J-715 spectropolarimeter in the 750–250 nm range. The values of $\Delta\varepsilon$ (*i.e.* $\varepsilon_l - \varepsilon_r$) and $\varepsilon$ were calculated at the maximum concentration of the particular species obtained from potentiometric data.

## 3 Results and discussion

Protonation constants (log $\beta$, log $K$ values) for the peptides studied and comparable ligands are given in Tables 1 and 2. The first protonation constant, log $\beta_{HL}$, for the hexapeptide amides refers to protonation of the ε-amino nitrogen of the lysine residue (log $K$ = 10.45–10.19) and the values agree well with

**Table 1** Protonation constants for EVHHQK-$NH_2$, EVRHQK-$NH_2$ and comparable peptides at $T$ = 298 K and $I$ = 0.10 M ($KNO_3$)

| Peptide | log $\beta$ | | | | | log $K$ | | | | | |
|---|---|---|---|---|---|---|---|---|---|---|---|
| | HL | $H_2L$ | $H_3L$ | $H_4L$ | $H_5L$ | $NH_2$-Lys | $NH_2$ | N-Im | N-Im | $\gamma$-$CO_2^-$ | $CO_2^-$ |
| **EVHHQK-$NH_2$** | **10.45 ± 0.01** | **18.20 ± 0.01** | **24.86 ± 0.01** | **30.72 ± 0.01** | **34.21 ± 0.01** | **10.45** | **7.75** | **6.66** | **5.86** | **3.49** | |
| GGH[a] | 8.06 | 14.88 | 17.68 | | | | 8.06 | 6.82 | | | 2.80 |
| RTHGQ-$NH_2$[b] | 7.246 | 13.276 | | | | | 7.246 | 6.030 | | | |
| HmS-HmS-His-$NH_2$[c] | 6.636 | 12.322 | | | | | 6.636 | 5.686 | | | |
| **EVRHQK-$NH_2$** | **10.31 ± 0.01** | **17.89 ± 0.01** | **24.06 ± 0.01** | **27.60 ± 0.01** | | **10.31** | **7.58** | **6.17** | | **3.54** | |
| GGGH[d] | 8.03 | 14.89 | 17.55 | | | | 8.03 | 6.86 | | | 2.66 |
| AGGH[e] | 8.14 | 15.03 | 17.65 | | | | 8.14 | 6.89 | | | 2.62 |

[a] Ref. 30. [b] Ref. 31. [c] Ref. 32. [d] Ref. 33. [e] Ref. 34.

**Table 2** Protonation constants for Ac-EVHHQK-$NH_2$, Ac-EVRHQK-$NH_2$ and comparable peptides at 298 K and $I = 0.10$ M ($KNO_3$)

| Peptide | log $\beta$ | | | | log $K$ | | | | | |
|---|---|---|---|---|---|---|---|---|---|---|
| | HL | $H_2L$ | $H_3L$ | $H_4L$ | $NH_2$-Lys | $NH_2$-Lys | N-Im | $\gamma$-$CO_2^-$ | $CO_2^-$ | $O^-$-Tyr |
| **Ac-EVHHQK-$NH_2$** | **10.39 ± 0.01** | **17.21 ± 0.01** | **23.15 ± 0.01** | **27.07 ± 0.01** | **10.39** | | **6.82** | **5.94** | **3.92** | |
| Ac-GGH[a] | 7.18 | 10.26 | | | | | 7.18 | | | 3.08 | |
| Ac-YIH[b] | 9.78 | 16.80 | 19.74 | | | | 7.02 | | | 2.94 | 9.78 |
| **Ac-EVRHQK-$NH_2$** | **10.19 ± 0.01** | **16.45 ± 0.01** | **20.49 ± 0.01** | | **10.19** | | | **6.26** | **4.04** | |
| Ac-AKRHRK-$NH_2$[c] | 11.03 | 20.90 | 27.03 | | 11.03 | 9.87 | | 6.13 | | |

[a] Ref. 35. [b] Ref. 36. [c] Ref. 37.

literature data.[28] Two of the hexapeptide amides, EVHHQK-$NH_2$ and EVRHQK-$NH_2$, have a free amino group and the stepwise protonation constants with log $K = 7.75$, 7.58 correspond very well to protonation of the N-terminal amino nitrogen. These values are comparable with that for the EAAA peptide (log $K = 7.77$) containing the same (glutamic acid) residue in the N-terminal position.[29] The human peptide amides (Ac-EVHHQK-$NH_2$, EVHHQK-$NH_2$) have two protonation constants (log $K = 6.82$, 5.94 and 6.66, 5.86, respectively) and the mouse peptide fragments (Ac-EVRHQK-$NH_2$, EVRHQK-$NH_2$) protonation constant (log $K = 6.26$ and 6.17, respectively, Tables 1 and 2) which correspond to protonation of the pyridine-like imidazole nitrogen of the His residue. These values are close to those expected for comparable peptides (Tables 1 and 2).[30–37] The protonation constants of the γ-carboxylate group of the Glu residue (log $K = 4.04$–3.49) in all ligands studied are close to those of peptides containing glutamic acid in their peptide sequence.[29]

Potentiometry detects a range of $Cu^{2+}$ complexes with the formation constants reported in Tables 3 and 4. The values of log $K^*$ are the protonation corrected stability constants which are useful to compare the ability of various ligands to bind a metal ion.[38,39] Spectroscopic properties of major complexes are given in Tables 5 and 6.

### $Cu^{2+}$–EVHHQK-$NH_2$ and –EVRHQK-$NH_2$ complexes

Five metal complex species can be fitted to the experimental titration curves obtained for the $Cu^{II}$–EVHHQK-$NH_2$ system: $CuH_3L$, CuHL, CuL, $CuH_{-1}L$ and $CuH_{-2}L$ (charges omitted for simplicity, Table 3). The coordination of metal ion starts at pH around 3.5 and the $CuH_3L$ complex is formed. As shown by potentiometry the $CuH_3L$ and CuHL complexes are minor species and cannot be characterized clearly by spectroscopy (Fig. 1). However the existence of the $CuH_3L$ complex has been confirmed by EPR spectroscopy. The EPR parameters $g_{\|} = 2.345$ and $A_{\|} = 138$ G are consistent with coordination of an imidazole nitrogen to copper(II) ions (Table 5).[34,36] The value of log $K^*$ for the 1N complex of EVHHQK-$NH_2$ peptide amide (−2.18, Table 3) is comparable to those obtained for peptides containing the His residue where the first complex may involve coordination of an imidazole-N donor center.[34] However, the $CuH_3L$ complex can be interpreted either by coordination of the terminal amino and neighboring carbonyl oxygen donors and the protonated imidazole side chain, or by monodentate coordination of an imidazole nitrogen and a protonated amino group, and therefore there is a possibility of the formation of bonding isomers in the solution.

In the pH range 4.5–10.5 the CuL, $CuH_{-1}L$ and $CuH_{-2}L$ species are formed (Fig. 1). Spectroscopic parameters in this pH

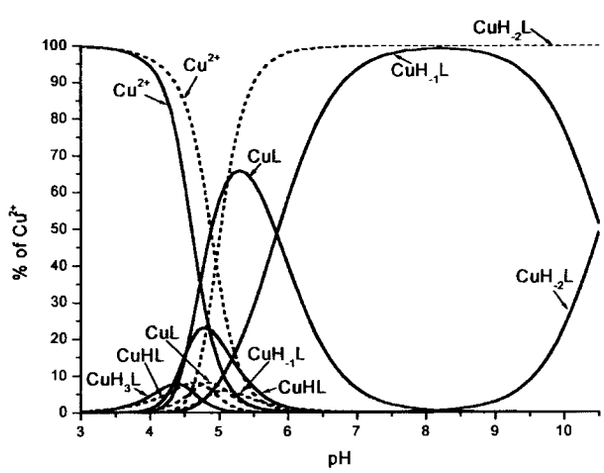


**Fig. 1** Species distribution curves for $Cu^{2+}$ complexes of GGH (dotted lines) and EVHHQK-$NH_2$ (solid lines). $Cu^{2+}$-to-peptide molar ratio 1 : 1, $[Cu^{II}] = 0.001$ M.

**Table 3** Stability constants of copper(II) complexes of EVHHQK-$NH_2$, EVRHQK-$NH_2$ and comparable peptides (concentration constants at 298 K and $I = 0.10$ M ($KNO_3$)

| | log $\beta$ | | | | | | |
|---|---|---|---|---|---|---|---|
| Peptide | $CuH_3L$ | $CuH_2L$ | CuHL | CuL | $CuH_{-1}L$ | $CuH_{-2}L$ | $CuH_{-3}L$ |
| **EVHHQK-$NH_2$** | **28.54 ± 0.03** | | **19.86 ± 0.01** | **15.32 ± 0.01** | **9.48 ± 0.01** | **−1.04 ± 0.01** | |
| GGH [a] | | | 12.40 | 7.64 | 2.55 | −1.55 | |
| RTHGQ-$NH_2$ [b] | | | | | | −0.96 | −10.34 |
| HmS-HmS-His-$NH_2$ [c] | | | | | 4.09 | 1.271 | −10.15 |
| **EVRHQK-$NH_2$** | | **21.42 ± 0.04** | **16.45 ± 0.01** | **10.23 ± 0.01** | **3.58 ± 0.01** | **−5.11 ± 0.01** | **−15.41 ± 0.02** |
| GGGH [d] | | | 12.24 | 8.47 | 1.63 | −5.79 | −16.67 |
| AGGH [e] | | | 12.72 | 8.43 | 1.82 | −5.36 | −15.24 |

| log $K^*$ vaules [f] | 1N ($N_{Im}$ or $NH_2$) | 2N ($NH_2$, CO, $N_{Im}$) | 3N ($NH_2$, $N^-$, CO, $N_{Im}$) | 4N ($NH_2$, $2N^-$, $N_{Im}$) | 4N ($NH_2$, $3N^-$) |
|---|---|---|---|---|---|
| **EVHHQK-$NH_2$** | **−2.18** | | **−10.86** | **−15.40** | |
| GGH | −2.48 | −7.24 | −12.33 | −16.43 | |
| RTHGQ-$NH_2$ | | | | −14.24 | |
| HmS-HmS-His-$NH_2$ | | | −8.232 | −11.05 | |
| **EVRHQK-$NH_2$** | **−2.64** | **−7.61** | **−13.83** | **−20.48** | **−23.00** |
| GGGH | −2.65 | −6.42 | −13.26 | −20.68 | −24.70 |
| AGGH | −2.31 | −6.60 | −13.21 | −20.39 | −23.38 |

Values for the ionization of the first, second and third amide groups

| | p$K_1$(amide) | p$K_2$(amide) | p$K_3$(amide) |
|---|---|---|---|
| **EVRHQK-$NH_2$** | **6.22** | **6.65** | **8.69** |
| GGGH | 6.84 | 7.42 | 10.88 |
| AGGH | 6.61 | 7.18 | 9.88 |

[a] Ref. 30. [b] Ref. 31. [c] Ref. 32. [d] Ref. 33. [e] Ref. 34. [f] log $K^*$ = log $\beta(CuH_jL)$ − log $\beta(H_nL)$ ($H_4L$ with EVHHQK-$NH_2$; $H_2L$ with GGH, RTHGQ-$NH_2$, HmS-HmS-His-$NH_2$, AGGH-OMe; $H_3L$ or $H_2L$ with EVRHQK-$NH_2$; and $H_2L$ or HL with GGGH, AGGH).

**Table 4** Stability constants of copper(II) complexes of Ac-EVHHQK-$NH_2$, Ac-EVRHQK-$NH_2$ and comparable peptides (concentration constants at 298 K and $I = 0.10$ M ($KNO_3$))

| | log $\beta$ | | | | | |
|---|---|---|---|---|---|---|
| Peptide | $CuH_2L$ | CuHL | CuL | $CuH_{-1}L$ | $CuH_{-2}L$ | $CuH_{-3}L$ |
| **Ac-EVHHQK-$NH_2$** | **21.03 ± 0.01** | **16.21 ± 0.01** | **10.18 ± 0.01** | **2.86 ± 0.01** | **−6.31 ± 0.01** | **−16.72 ± 0.01** |
| Ac-GGH [a] | | | 4.24 | −2.26 | −9.61 | −18.86 |
| Ac-YIH [b] | | 14.26 | 7.27 | −0.07 | −8.99 | −18.95 |
| **Ac-EVRHQK-$NH_2$** | | **14.01 ± 0.01** | | **1.93 ± 0.01** | **−6.66 ± 0.01** | **−16.83 ± 0.01** |
| Ac-AKRHRK-$NH_2$ [c] | 23.70 | | 12.45 | 3.98 | −5.94 | −16.92 |

| log $K^*$ values [d] | 1N ($N_{Im}$) | 2N ($N_{Im}$, $N^-$) | 3N ($N_{Im}$, $2N^-$) | 4N ($N_{Im}$, $3N^-$) |
|---|---|---|---|---|
| **Ac-EVHHQK-$NH_2$** | **−2.12** | **−7.03** | **−14.35** | **−23.52** |
| Ac-GGH | −2.94 | −9.44 | −16.79 | −26.04 |
| Ac-YIH | −2.54 | −9.53 | −16.87 | −25.79 |
| **Ac-EVRHQK-$NH_2$** | **−2.44** | | **−14.52** | **−23.11** |
| Ac-AKRHRK-$NH_2$ | −3.33 | | −14.58 | −23.05 |

Values for ionization of the first, second and third amide groups

| | p$K_1$(amide) | p$K_2$(amide) | p$K_3$(amide) |
|---|---|---|---|
| **Ac-EVHHQK-$NH_2$** | **6.03** | **7.32** | **9.17** |
| Ac-GGH | 6.50 | 7.35 | 9.25 |
| Ac-YIH | 6.99 | 7.34 | 8.92 |
| **Ac-EVRHQK-$NH_2$** | | | **8.59** |
| Ac-AKRHRK-$NH_2$ | | | 8.47 |

[a] Ref. 35. [b] Ref. 36. [c] Ref. 37. [d] log $K^*$ = log $\beta(CuH_jL)$ − log $\beta(H_nL)$ ($H_2L$ with Ac-EVRHQK-$NH_2$, Ac-YIH; HL with Ac-GGH, Boc-AGGH; $H_3L$ with Ac-AKRHRK-$NH_2$ and Ac-EVHHQK-$NH_2$ for $CuH_2L$ but $H_2L$ for CuL, $CuH_{-1}L$ and $CuH_{-2}L$ species).

range indicate similar bonding mode in these complexes (Table 5). The EPR parameters $g_{\|} = 2.184$–$2.178$ and $A_{\|} = 204$ G, the d–d transition energy at 520–517 nm and the presence in CD spectra of the $N^-_{amide} \rightarrow Cu^{2+}$ and $NH_2 \rightarrow Cu^{2+}$ charge transfer transitions at 315–314 and 276–273 nm (respectively) correspond to the four nitrogen {$NH_2$, $2N^-$, $N_{Im}$} coordination

**Table 5** Spectroscopic data for copper(II) complexes of EVHHQK-$NH_2$ and EVRHQK-$NH_2$

| | UV-vis | | CD | | EPR | |
|---|---|---|---|---|---|---|
| Ligand/species | $\lambda$/nm | $\varepsilon$/$M^{-1}$ $cm^{-1}$ | $\lambda$/nm | $\Delta\varepsilon$/$M^{-1}$ $cm^{-1}$ | $A_\parallel$/G | $g_\parallel$ |
| EVHHQK-$NH_2$ | | | | | | |
| $CuH_3L$ "1N"{$N_{Im}$ or $NH_2$} | | | | | 138 | 2.345 |
| CuL "4N"{$NH_2$, $2N^-$, $N_{Im}$} | 517[a] | 130 | 557[a] | −1.137 | 204 | 2.178 |
| | | | 481[a] | +0.489 | | |
| | | | 314[b] | +1.951 | | |
| | | | 273[c] | −3.843 | | |
| $CuH_{-1}L$ "4N"{$NH_2$, $2N^-$, $N_{Im}$} | 520[a] | 109 | 557[a] | −1.125 | 204 | 2.182 |
| | | | 480[a] | +0.516 | | |
| | | | 315[b] | +1.845 | | |
| | | | 276[c] | −3.812 | | |
| $CuH_{-2}L$ "4N"{$NH_2$, $2N^-$, $N_{Im}$} | 520[a] | 101 | 555[a] | −1.318 | 204 | 2.184 |
| | | | 477[a] | +0.401 | | |
| | | | 314[b] | +2.061 | | |
| | | | 274[c] | −3.642 | | |
| EVRHQK-$NH_2$ | | | | | | |
| $CuH_2L$ "1N"{$N_{Im}$ or $NH_2$} | 749[a] | 41 | | | 150 | 2.330 |
| CuHL "2N"{$NH_2$, CO, $N_{Im}$} | 669[a] | 78 | | | 146 | 2.296 |
| CuL "3N"{$NH_2$, $N^-$, CO, $N_{Im}$} | 593[a] | 96 | 581[a] | −0.346 | | |
| | | | 326[b,d] | +1.105 | | |
| | | | 287[c] | −1.318 | | |
| $CuH_{-1}L$ "4N"{$NH_2$, $2N^-$, $N_{Im}$} | 553[a] | 120 | 569[a] | −0.900 | 195 | 2.198 |
| | | | 331[b,d] | +1.797 | | |
| | | | 288[c] | −3.552 | | |
| $CuH_{-2}L$ "4N"{$NH_2$, $3N^-$} | 514[a] | 158 | 518[a] | −2.008 | 199 | 2.189 |
| | | | 316[b] | +1.741 | | |
| | | | 275[c] | −3.481 | | |
| $CuH_{-3}L$ "4N"{$NH_2$, $3N^-$} | 511[a] | 160 | 516[a] | −2.566 | 204 | 2.181 |
| | | | 311[b] | +2.180 | | |
| | | | 276[c] | −3.655 | | |

[a] d–d transition. [b] $N^-_{amide}\rightarrow Cu^{2+}$ charge transfer transition. [c] $NH_2\rightarrow Cu^{2+}$ charge transfer transition. [d] $N_{Im}\rightarrow Cu^{2+}$ charge transfer transition.

mode (Table 5).[32] This bonding mode is identical to that of complexes of Gly-Gly-His and other Xaa-Yaa-His peptides.[31,32] Two deprotonations, $CuL \longrightarrow CuH_{-1}L \longrightarrow CuH_{-2}L$, correspond to deprotonations of imidazole nitrogen, the fourth histidine and of ε-amino nitrogen lysine residues. The protonation constants of the $CuH_{-2}L$ complex (10.52) and of the $CuH_{-1}L$ complex (5.84) are in good agreement with those for protonations of the Lys and His residues in the "free" ligand (10.45; 5.86 respectively, Tables 1 and 3). Values of log $K$* for complexes with 4N coordination are shown in Table 3 and these suggest a stabilization of $Cu^{2+}$–EVHHQK-$NH_2$ complex by about one order of magnitude compared to that of Gly-Gly-His, but this value for the ligand studied is four orders of magnitude less compared to that of HmS-HmS-His-$NH_2$ (HmS = α-hydroxymethylserine). The studies indicate that the very acidic ammonium group of the HmS residue changes distinctly the electron density within the amide bond causing the amide nitrogen to become a much more effective donor than nitrogens derived from amino acids with more basic amino functions. This unusual gain in the 4N complex stability in the copper(II)–HmS-HmS-His-$NH_2$ complex seems to derive from enhancement of the π-electron contribution to the metal–amide nitrogen bond.[40]

From potentiometric data calculations six monomeric complexes are found for the $Cu^{II}$–EVRHQK-$NH_2$ (11–16M) system: $CuH_2L$, CuHL, CuL, $CuH_{-1}L$, $CuH_{-2}L$ and $CuH_{-3}L$ (Table 3, Fig. 2). The $CuH_2L$ species may be regarded as comparable to the CuHL complex of GGGH with an additional protonated ε-amino residue (on $Lys^6$). Earlier studies led to the conclusions that the nitrogen ($N^3$) of imidazole is the primary bonding site of these peptides.[34,41,42] The comparison of the EPR parameters for $CuH_2L$ complex ($A_\parallel$ = 150 G, $g_\parallel$ = 2.330, Table 5) to that for 1N complex of pentaglycine may suggest the existence of amine bonding.[33] However, the EPR parameters obtained for $Cu^{2+}$–Ac-EVRHQK-$NH_2$ (amino group is blocked by acetylation, see below), for the first complex formed with the imidazole nitrogen coordination ($A_\parallel$ = 149 G and $g_\parallel$ = 2.336, Table 6), are comparable to those of EVRHQK-$NH_2$. This comparision suggests that coordination of the copper(II) ions to EVRHQK-$NH_2$ peptide may start from the amine group or the imidazole nitrogen of the histidine residue.

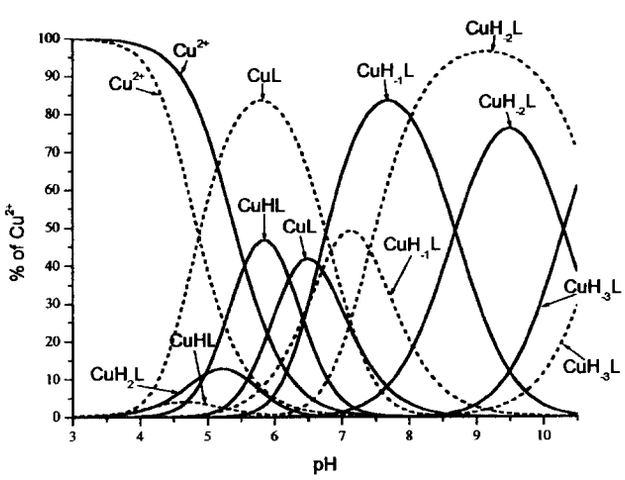


**Fig. 2** Species distribution curves for $Cu^{2+}$ complexes of GGGH (dotted lines) and EVRHQK-$NH_2$ (solid lines). Details as in Fig. 1.

With increasing pH above 4.5 the CuHL complex is formed with p$K$ value for deprotonation of the $CuH_2L$ species ($CuH_2L \rightleftharpoons CuHL + H^+$) equal 4.97. The formation of CuHL is accompanied by a significant blue shift of the absorption band to 669 nm suggesting coordination of the additional nitrogen donor (Table 5). The EPR parameters for the CuHL complex, $A_\parallel$ = 146 G and $g_\parallel$ = 2.296, are comparable to those of AGGH[34] and GGGH.[33] The value for $A_\parallel$ is distinctly lower

**Table 6** Spectroscopic data for copper(II) complexes of Ac-EVHHQK-$NH_2$ and Ac-EVRHQK-$NH_2$

| | UV-vis | | CD | | EPR | |
|---|---|---|---|---|---|---|
| Ligand/species | $\lambda$/nm | $\varepsilon$/$M^{-1}$ $cm^{-1}$ | $\lambda$/nm | $\Delta\varepsilon$/$M^{-1}$ $cm^{-1}$ | $A_{\parallel}$/G | $g_{\parallel}$ |
| Ac-EVHHQK-$NH_2$ | | | | | | |
| CuHL "2N"{$N_{Im}$, $N_{Im}$} | 620[a] | 57 | | | 157 | 2.312 |
| CuL "3N"{$N_{Im}$, $N^-$, $N_{Im}$} | 593[a] | 119 | 568[a] | +0.794 | 182 | 2.238 |
| | | | 344[b] | −0.175 | | |
| | | | 292sh[c] | +2.320 | | |
| | | | 256[d] | +4.340 | | |
| $CuH_{-1}L$ "3N"{$N_{Im}$, $2N^-$} | 588[a] | 100 | 543[a] | +0.299 | 167 | 2.235 |
| | | | 355[b] | −0.615 | | |
| | | | 265[d] | +5.134 | | |
| $CuH_{-2}L$ "4N"{$N_{Im}$, $3N^-$} | 522[a] | 99 | 640[a] | +0.868 | 209 | 2.180 |
| | | | 495[a] | −1.531 | | |
| | | | 360[b] | −0.517 | | |
| | | | 312[c] | +1.342 | | |
| | | | 257[d] | +9.505 | | |
| $CuH_{-3}L$ "4N"{$N_{Im}$, $3N^-$} | 518[a] | 109 | 643[a] | +1.234 | 204 | 2.183 |
| | | | 495[b] | −2.520 | | |
| | | | 360[b] | −0.415 | | |
| | | | 315[c] | +1.891 | | |
| | | | 261[d] | +10.381 | | |
| Ac-EVRHQK-$NH_2$ | | | | | | |
| CuHL "1N"{$N_{Im}$} | 742[a] | 49 | | | 149 | 2.336 |
| $CuH_{-1}L$ "3N"{$N_{Im}$, $2N^-$} | 597[a] | 87 | 540[a] | +0.614 | 163 | 2.235 |
| | | | 342[b,c] | −0.841 | | |
| | | | 247[d] | +8.262 | | |
| $CuH_{-2}L$ "4N"{$N_{Im}$, $3N^-$} | 516[a] | 102 | 641[a] | +1.003 | 209 | 2.180 |
| | | | 490[a] | −1.827 | | |
| | | | 359[b] | −0.442 | | |
| | | | 315[c] | +2.237 | | |
| | | | 262[d] | +9.486 | | |
| $CuH_{-3}L$ "4N"{$N_{Im}$, $3N^-$} | 515[a] | 105 | 642[a] | +1.063 | 200 | 2.182 |
| | | | 492[a] | −2.069 | | |
| | | | 360[b] | −0.431 | | |
| | | | 314[c] | +2.468 | | |
| | | | 262[d] | +9.486 | | |

[a] d–d transition. [b] $N_{Imd}\rightarrow Cu^{2+}$ charge transfer transition. [c] $N^-_{amide}\rightarrow Cu^{2+}$ charge transfer transition. [d] $N_{Im}$ $\pi_2\rightarrow Cu^{2+}$ charge transfer transition.

than for the other 2N species which form typical, small, chelate rings.[33] Such changes in $A_{\parallel}$ may reflect deformation of the complex plane expected when a macrochelate ring spanning the terminal $NH_2$ and $N_{Im}$ donor centers is formed. A similar mode of coordination {$NH_2$, CO, $N_{Im}$} for similar complexes was suggested many years ago.[43] The CuL, $CuH_{-1}L$ and $CuH_{-2}L$ complexes are formed by sequential deprotonation and coordination of peptide nitrogens. The value of 593 nm for the d–d band energy of the CuL species is a little above that typical of 3N complexes of simple peptides (*ca.* 570 nm) but can easily be explained when ligand effects are taken into account since these are in the order $N_{Im} < NH_2 < N^-_{amide}$.[44] As a result a 3N species involving $N_{Im}$, $NH_2$, $N^-$ coordination would be expected to have a higher value for $\lambda_{max}$ than a 3N species involving $Cu^{2+}$–$NH_2$ and two $Cu^{2+}$–$N^-$ bonds. In pH range 7–8.5 the $CuH_{-1}L$ species is detected as a major complex (Fig. 2). The EPR parameters $A_{\parallel} = 195$ G and $g_{\parallel} = 2.198$, the d–d transition energy at 553 nm and the presence in the CD spectrum of the $N_{Im}\rightarrow Cu^{2+}$ charge transfer transition at 331 nm are consistent with 4N {$NH_2$, $2N^-$, $N_{Im}$} coordination of the peptide amide to copper(II) ions (Table 5).[33] Coordination of histidine normally gives charge transfer transitions at *ca.* 330 nm [$\pi_1(N_{Im}$–$Cu^{2+})$]. The magnitude and precise energy of the charge transfer transitions for an imidazole nitrogen to $Cu^{2+}$ are very sensitive to the position of the ring plane relative to the complex plane, and thus to the possibility of its rotation.[45] The charge transfer transition $N^-_{amide}\rightarrow Cu^{2+}$ is also located around 310–320 nm, making it impossible to use these bands to conclude whether or not the imidazole is involved in complexation. However, the presence of this band at 330 nm may suggest the involvement of the imidazole nitrogen in the coordination of copper(II) ion. The $CuH_{-1}L$ species is a 4N complex. The copper(II) ion is coordinated by amino nitrogen, two amide nitrogens from the N-terminal side and the fourth coordination site is occupied by the imidazole group. This coordination mode was suggested for GGGH.[33] Above pH 7 deprotonation and coordination of the third amide nitrogen takes place in the formation of the $CuH_{-2}L$ species. The d–d transition energy at 514 nm, the EPR parameters $A_{\parallel} = 199$ G and $g_{\parallel} = 2.189$ and the presence in the CD spectrum of charge transfer transitions $NH_2\rightarrow Cu^{2+}$, $N^-_{amide}\rightarrow Cu^{2+}$ indicate a 4N complex with {$NH_2$, $3N^-$} coordination mode. The replacement of imidazole bonding by the coordination of an amide nitrogen was suggested for the $Cu^{2+}$–KLAHFG system[46] and $Cu^{2+}$–GGGH.[33] Further deprotonation, $CuH_{-2}L \rightleftharpoons CuH_{-3}L + H^+$, corresponds to deprotonation of the lysine side chain. The protonation constant of the $CuH_{-3}L$ complex (10.30) is in good agreement to that for protonation of the lysine residue in the free ligand (10.31, Tables 1 and 3). The $CuH_{-3}L$ complex has very similar CD and EPR parameters to those of $CuH_{-2}L$, supporting no variation in the coordination mode during this deprotonation (Table 5). The different spectroscopic parameters (especially CD spectra) for the $Cu^{2+}$–EVRHQK-$NH_2$ (11–16M) system in comparison to $Cu^{2+}$–Ac-EVRHQK-$NH_2$ (Ac-11–16M) clearly indicate involvement of the amino group in the coordination of copper(II) ions (Tables 5 and 6).The log $K$* values for 3N and 4N {$NH_2$, $2N^-$, $N_{Im}$} complexes for the system studied are comparable to those of GGGH and AGGH (Table 3). The ionization (p$K_3$(amide) value) of the third amide nitrogen in the $Cu^{2+}$–EVRHQK-$NH_2$ system is about two orders of magnitude lower compared to that for GGGH (Table 3).

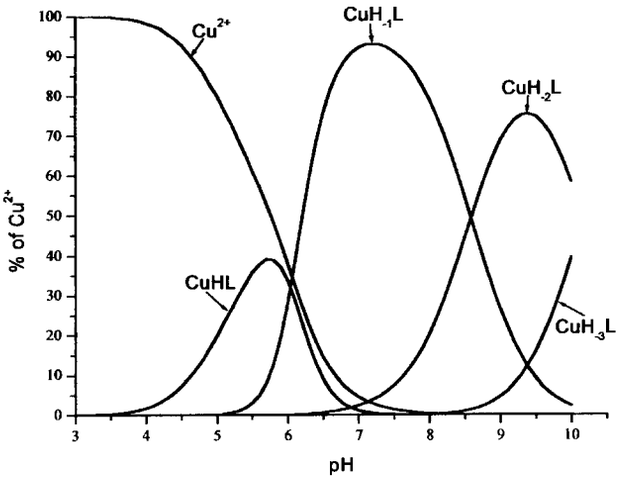


**Fig. 3** Species distribution curves for $Cu^{2+}$ complexes of Ac-EVRHQK-$NH_2$. Details as in Fig. 1.

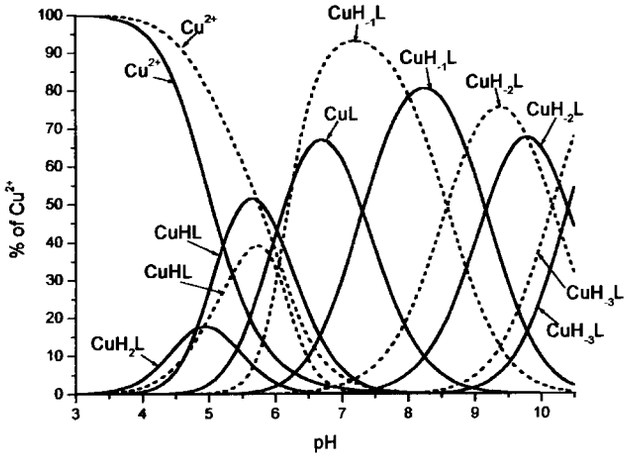


**Fig. 4** Species distribution curves for $Cu^{2+}$ complexes of Ac-EVRHQK-$NH_2$ (dotted lines) and Ac-EVHHQK-$NH_2$ (solid lines). Details as in Fig. 1.

### $Cu^{2+}$–Ac-EVHHQK-$NH_2$ and –Ac-EVRHQK-$NH_2$ complexes

According to potentiometric and spectroscopic results, the N-blocked hexapeptide amide Ac-EVRHQK-$NH_2$, the mouse fragment (Ac-11–16M) of the β-amyloid peptide, forms with $Cu^{2+}$ ions the CuHL, $CuH_{-1}L$, $CuH_{-2}L$ and $CuH_{-3}L$ species (Table 4, Fig. 3). The first complex CuHL with d–d transition at 742 nm and EPR parameters $A_{\parallel} = 149$ G, $g_{\parallel} = 2.336$ is the 1N complex with the imidazole nitrogen bound to the metal ion (Table 6).[32,34] With increasing pH, the CuHL complex loses two amide protons to give a species of stoichiometry $CuH_{-1}L$, reaching maximum concentration at pH ≈ 7.3 (Fig. 3). The EPR parameters $A_{\parallel} = 163$ G and $g_{\parallel} = 2.235$ and d–d transition energy of 597 nm are consistent with 3N coordination $\{N_{Im}, 2N^-\}$ of the peptide amide to copper(II) ion (Table 6).[37] Similar EPR parameters were observed for the 3N complex $\{N_{Im}, 2N^-\}$ of a 14-amino acid sequence of Cap 43 protein ($A_{\parallel} = 167$ G, $g_{\parallel} = 2.233$).[47] The low values of $A_{\parallel}$ obtained for these complexes may suggest distortion of the tetragonal geometry around the metal ion. At pH above 7 the $CuH_{-2}L$ and $CuH_{-3}L$ species are formed which have four nitrogen donor centers arranged in a square planar geometry around the central copper(II) ion. The spectroscopic parameters for these complexes are very similar suggesting the same coordination mode (Table 6). The shift of the absorption maximum to 516–515 nm and the EPR parameters $A_{\parallel} = 209$–$200$ G, $g_{\parallel} = 2.180$–$2.182$ suggest coordination of the additional nitrogen donor atom (Table 6).[37,48] The presence in the CD spectra of $N_{Im} \rightarrow Cu^{2+}$ and $N^-_{amide} \rightarrow Cu^{2+}$ charge transfer transitions at ≈360 and ≈314 nm, respectively, may suggest the coordination mode $\{N_{Im}, 3N^-\}$ in the $CuH_{-2}L$ and $CuH_{-3}L$ species. The protonation constant of the $CuH_{-3}L$ complex (10.17) is in good agreement to that for protonation of the lysine residue in the free peptide amide (10.19, Tables 2 and 4). supporting the various protonation states of the side chain lysine residue in the $CuH_{-2}L$ and $CuH_{-3}L$ complexes. The imidazole nitrogen acts as a metal ion anchoring group, while three amide nitrogens complete the coordination of copper(II) ion. The deprotonation and coordination of the two first amide nitrogens occur almost simultaneously and the 2N species was not detected (Table 4, Fig. 3). The log $K^*$ values of the 3N and 4N complexes formed by the mouse fragment (Ac-11–16M) of β-amyloid peptide in comparision with those for Ac-AKRHRK-$NH_2$ hexapeptide amide[37] and the values for ionization of the third amide nitrogen are comparable (Table 4).

Computer analysis of the potentiometric data has revealed the presence of the following species in the $Cu^{2+}$–Ac-EVHHQK-$NH_2$ system: $CuH_2L$, CuHL, CuL, $CuH_{-1}L$, $CuH_{-2}L$ and $CuH_{-3}L$ (Table 4). The $CuH_2L$ species is in low concentration thus the first detectable by spectroscopy is CuHL (Fig. 4). The protonation constant of the CuHL species is equal to 4.82 and is comparable to that for peptides with imidazole nitrogen coordination (Table 4).[34,36] The d–d transition energy at 620 nm and the EPR parameters $A_{\parallel} = 157$ G, $g_{\parallel} = 2.312$ are consistent with 2N $\{N_{Im}, N_{Im}\}$ coordination.[48] Similar EPR values were observed for a complex of copper(II) coordinated by two molecules of imidazole ($A_{\parallel} = 156$ G, $g_{\parallel} = 2.312$).[49] The coordination of the N-blocked hexapeptide amide to copper(II) ion starts from the imidazole nitrogen ($CuH_2L$ species), followed by the second imidazole nitrogen of the histidine residue giving CuHL. Additional evidence that two histidines are involved in coordination was obtained by $^1H$ NMR spectroscopy. The two resonances associated with the C(2)H and C(4)H imidazole protons of the two histidine residues are separated in the absence of metal ions at pH 5.6 (Fig. 5). When copper(II) ions are added in metal to ligand molar ratio 1 : 100 these resonances undergo line broadening and the spin–lattice relaxation rates of these protons are the most affected: rates for C(2)H and C(4)H for the metal free solution at pH 5.6 and at 298 K are 0.769 and 0.713 $s^{-1}$, respectively; when the copper(II) ions are added the relaxation rates increase to 28.728 and 31.672 $s^{-1}$ for a metal to ligand molar ratio 1 : 100 and to 60.599 and 57.003 $s^{-1}$ for a 1 : 50 molar ratio, respectively, supporting interaction of copper(II) ions with the imidazole nitrogen donors. The NMR method has also been used for the determination of the coordination mode in similar systems with copper(II) ions.[50,51]

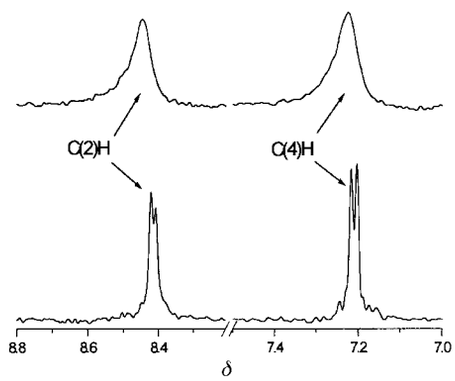


**Fig. 5** Downfield region of the 500 MHz $^1H$ NMR spectra of Ac-EVHHQK-$NH_2$ (0.002 M in $^2H_2O$, pH 5.6) in the absence (lower trace) and presence of $Cu^{2+}$. Metal to ligand molar ratio 1 : 100; C–H protons of the two histidines are indicated.

With increasing pH the CuL complex is formed with maximum concentration at pH ≈ 6.7 (Fig. 4). The deprotonation constant for $CuHL \rightleftharpoons CuL + H^+$ is equal to −6.03 and can

be assigned to deprotonation and coordination of the amide nitrogen (Table 4). The shift of the d–d transition energy to 593 nm, the presence in the CD spectrum of charge transfer transitions $N_{Im}\rightarrow Cu^{2+}$ at 344 nm, $N^-_{amide}\rightarrow Cu^{2+}$ at 292 nm and the EPR parameters $A_{\parallel} = 182$ G, $g_{\parallel} = 2.238$ may support formation of a 3N complex with $\{N_{Im}, N^-, N_{Im}\}$ coordination.[47] The high value of $A_{\parallel}$ may suggest coordination of the three nitrogens $\{N_{Im}, N^-, N_{Im}\}$ in the equatorial plane. Two imidazole nitrogens are coordinated in *trans* position to each other, while the amide nitrogen derives from His[4]. Tridentate coordination involving one amide nitrogen is supported by the low log $K_1$(amide) value (about one log unit less compared to Ac-YIH, Table 4). Above pH 6 the imidazole nitrogen of His[3] is replaced by the second amide nitrogen of His[3] and a 3N $\{N_{Im}, 2N^-\}$ complex is formed (see below). The log $K^*$ value for the CuL complex is about 2.5 orders of magnitude higher in comparison to that of Ac-GGH and Ac-YIH (Table 4). This increase may be explained by the coordination of the second histidine residue.

The CD, EPR and absorption spectroscopic parameters for the $CuH_{-1}L$ species are consistent with a 3N $\{N_{Im}, 2N^-\}$ coordination mode[48] and are comparable to those of the $CuH_{-1}L$ complex of the mouse fragment, Ac-EVRHQK-$NH_2$. The deprotonation constant of the CuL complex (−7.32) corresponds very well to deprotonation and coordination of the second amide nitrogen to copper(II) (Table 4). The log $K^*$ value for the 3N complex $\{N_{Im}, 2N^-\}$ is comparable to that of the mouse fragment, Ac-EVRHQK-$NH_2$, suggesting the same coordination mode.

At higher pH the next deprotonation and coordination of the amide nitrogen occur and the $CuH_{-2}L$ complex is formed with maximum concentration at pH ≈ 9.6 (Fig. 4). The p$K_3$(amide) value (9.17) for the N-blocked hexapeptide amide studied is comparable to that of Ac-GGH and Ac-YIH, supporting involvement of the next amide nitrogen in coordination (Table 4). This suggestion is confirmed by the CD, EPR and UV-Vis spectroscopic parameters. The d–d transition energy at 522 nm, the presence in the CD spectrum of charge transfer transitions $N_{Im}\rightarrow Cu^{2+}$, $N^-_{amide}\rightarrow Cu^{2+}$ at 360 and 312 nm, respectively, and the EPR parameters $A_{\parallel} = 209$ G, $g_{\parallel} = 2.180$ are in good accordance with 4N $\{N_{Im}, 3N^-\}$ coordination. These spectroscopic parameters are comparable to those of the $CuH_{-2}L$ species with the mouse fragment Ac-EVRHQK-$NH_2$ (Ac-11–16M), supporting the same coordination mode (Table 6). The log $K^*$ value (−23.52) for this complex is comparable to that for the mouse fragment (−23.11), Ac-EVRHQK-$NH_2$ peptide amide (Table 4).

The next deprotonation (resulting in the $CuH_{-3}L$ species) has no effect on the structure of the complex formed, as seen from the CD, EPR and UV-Vis measurements (Table 6). It must in fact be due to deprotonation of the non-coordinated ε-amino group of the lysine residue. The protonation constant of the $CuH_{-3}L$ complex (10.41) corresponds very well to that in free ligand (10.39, Tables 2 and 4).

To visualize the chelation ability of the human fragment in comparison with the mouse fragment of β-amyloid peptide a competition plot was made by taking into account the stability constants for the $Cu^{2+}$–Ac-EVHHQK-$NH_2$ and $Cu^{2+}$–Ac-EVRHQK-$NH_2$ systems (Fig. 6). The calculations were made assuming a 1:1:1 $Cu^{II}$:Ac-EVHHQK-$NH_2$:Ac-EVRHQK-$NH_2$ molar ratio. The plot obtained for $Cu^{2+}$ clearly indicates that in a wide pH range including physiological pH the human fragment (Ac-11–16H) of β-amyloid peptide is much more effective in metal ion bonding than is the mouse fragment.

## Conclusion

The hexapeptide amide EVHHQK-$NH_2$ containing the N-terminal sequence Xaa-Yaa-His forms in pH range 4.5–10.5 very stable complexes typical for this sequence. The imidazole nitrogen of the second histidine residue does not take part in the coordination. The mouse fragment of β-amyloid peptide EVRHQK-$NH_2$ containing in its fourth position a histidine residue, in a wide pH range including the physiological pH, is coordinated to copper(II) ion through the N-terminal amino group, the imidazole nitrogen of histidine and an increasing number of deprotonated amide nitrogens in the form of a macrochelate. The imidazole nitrogen leaves the coordination sphere of the copper(II) ion only above *ca.* pH 7, allowing the formation of classical peptide type coordination starting from the N-terminal amino group up to the third deprotonated amide group as in the case of peptides with non-coordinating side chains. The acetylation of the N-terminal amino group has a major influence on both the speciation and structures of the complexes formed. The coordination of the mouse fragment Ac-EVRHQK-$NH_2$ (Ac-11–16M) starts from the imidazole nitrogen of the histidine residue and with increasing pH sequential amide nitrogens are coordinated. The imidazole nitrogen of the histidine residue acts also as an anchoring bonding site for the human fragment, Ac-EVHHQK-$NH_2$ (Ac-11–16H). In a wide pH range, $Cu^{II}$ is bound to the peptide through imidazole nitrogens on both of its histidine residues and with increasing pH sequential amide nitrogens are also bound. At pH above *ca.* 6 the imidazole nitrogen leaves the coordination sphere of the copper(II) ion and 3N and 4N complexes are formed. The competition plot clearly indicates that, in a wide pH range including physiological pH, Ac-EVHHQK-$NH_2$ (human fragment, Ac-11–16H) is more effective in copper(II) bonding than is Ac-EVRHQK-$NH_2$ (mouse fragment, Ac-11–16M) because of the presence of the His-His sequence in the human fragment of β-amyloid peptide.

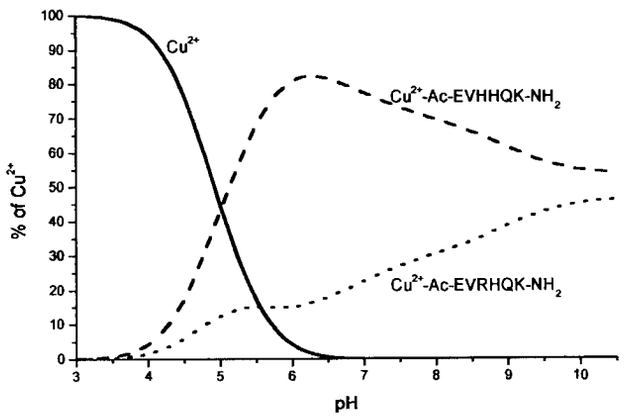


**Fig. 6** The distribution of $Cu^{2+}$ between Ac-EVHHQK-$NH_2$ and Ac-EVRHQK-$NH_2$ in aqueous solution for a molar ratio 1:1:1.


## Acknowledgements

This work was supported by the Polish State Committee for Scientific Research (KBN 3 T09A 069 18).


## References


1 J. Hardy, *Trends Neurosci.*, 1997, **20**, 154.
2 A. C. McKee, K. S. Kosik and N. W. Kowall, *Annu. Neurol.*, 1991, **30**, 156.
3 G. G. Glenner and C. W. Wang, *Biochem. Biophys. Res. Commun.*, 1984, **120**, 885.
4 J. Kang, H. G. Lemaire, A. Unterbeck, J. M. Salbaum, C. L. Masters, K. H. Grzeschik, G. Multhaup, K. Beyreuther and B. Muller-Hill, *Nature* (*London*), 1987, **325**, 733.
5 X. D. Cai, T. E. Golde and S. G. Younkin, *Science*, 1993, **259**, 514.
6 M. Citron, T. Oltersdorf, Ch. Haass, L. McConlogue, A. Y. Hung, P. Seubert, C. Vigo-Pelfrey, I. Lieberburg and D. J. Selkoe, *Nature* (*London*), 1992, **360**, 672.
7 N. Suzuki, T. T. Cheung, X.-D. Cai, A. Odaka, L. Otvos, Ch. Eckman, T. E. Golde and S. G. Younkin, *Science*, 1994, **264**, 1336.

8 B. D. Shivers, C. Hilbich, G. Multaup, M. Salbaum, K. Beyreuther and P. H. Seeburg, *Eur. Mol. Biol. Org. J.*, 1988, **7**, 1365.
9 T. Yamada, H. Sasaki, H. Furuya, T. Miyata, I. Goto and Y. Sakaki, *Biochem. Biophys. Res. Commun.*, 1987, **149**, 665.
10 T. Dyrks, E. Dyrks, C. L. Masters and K. Beyreuther, *FEBS Lett.*, 1993, **324**, 231.
11 L. J. Otvos, G. I. Szendrei, V. M. Lee and H. H. Mantsch, *Eur. J. Biochem.*, 1993, **211**, 249.
12 E. M. Johnstone, M. O. Chaney, F. H. Norris, R. Pascual and S. P. Little, *Mol. Brain Res.*, 1991, **10**, 299.
13 B. De Strooper, M. Simons, G. Multhaup, F. Van Leuven, K. Beyreuther and C. G. Dotti, *Eur. Mol. Biol. Org. J.*, 1995, **14**, 4932.
14 C. L. Joachim and D. L. Selkoe, *Alzheimer Dis. Assoc. Disord.*, 1992, **6**, 7.
15 A. R. White, R. Reyes, J. F. B. Mercer, J. Camakaris, H. Zheng, A. I. Bush, G. Multhaup, K. Beyreuther, C. L. Masters and R. Cappai, *Brain Res.*, 1999, **842**, 439.
16 C. S. Atwood, R. D. Moir, X. D. Huang, R. C. Scarpa, N. M. E. Bacarra, D. M. Romano, M. K. Hartshorn, R. E. Tanzi and A. I. Bush, *J. Biol. Chem.*, 1998, **2273**, 12817.
17 S. C. Bondy, S. X. Guo-Ross and A. T. Truong, *Brain Res.*, 1998, **799**, 91.
18 G. Multhaup, T. Ruppert, A. Schlicksupp, L. Hesse, E. Bill, R. Pipkorn, C. L. Masters and K. Beyreuther, *Biochemistry*, 1998, **37**, 7224.
19 X. Huang, C. S. Atwood, M. A. Hartshorn, G. Multhaup, L. E. Goldstein, R. C. Scarpa, M. P. Cuajung, D. N. Gray, J. Lim, R. D. Moir, R. E. Tanzi and A. I. Bush, *Biochemistry*, 1999, **38**, 7609.
20 M. A. Lovell, J. D. Robertson, W. J. Teesdala, J. L. Campbell and W. R. Markesbery, *J. Neurol. Sci.*, 1998, **158**, 47.
21 R. A. Cherny, T. J. Legg, C. A. McLean, D. Fairlie, X. Huang, C. S. Atwood, K. Beyreuther, R. E. Tanzi, C. L. Masters and A. I. Bush, *J. Biol. Chem.*, 1999, **274**, 23223.
22 X. Huang, M. P. Cuajungco, C. S. Atwood, M. A. Hartshorn, J. D. A. Tyndall, G. R. Hanson, K. C. Stokes, M. Leopold, G. Multhaup, L. E. Goldstein, R. C. Scarpa, A. J. Saunders, J. Lim, R. D. Moir, Ch. Glabe, E. F. Bowden, C. L. Masters, D. P. Fairlie, R. E. Tanzi and A. I. Bush, *J. Biol. Chem.*, 1999, **274**, 37111.
23 J. M. Steward and J. D. Young, *Solid Phase Peptide Synthesis*, Pierce Chemical Company, Rockford, IL, 1993.
24 *The Milliphore 9050 Plus PepSynthesizer Operator's Guide*, Milliphore Corporation, Milford, 1992.
25 N. Sole and G. Barany, *J. Org. Chem.*, 1992, **57**, 5399.
26 H. Irving, M. G. Miles and L. D. Pettit, *Anal. Chim. Acta*, 1967, **38**, 475.
27 P. Gans, A. Sabatini and A. Vacca, *J. Chem. Soc.*, *Dalton Trans.*, 1985, 1195.
28 I. Sovago, T. Kiss and A. Gergely, *Inorg. Chim. Acta*, 1984, **93**, L53.
29 J. F. Galey, B. Decock-Le Reverend, A. Lebkiri, L. D. Pettit, S. I. Pyburn and H. Kozłowski, *J. Chem. Soc.*, *Dalton Trans.*, 1991, 2281.
30 R. W. Hay, M. M. Hassan and C. You-Quan, *J. Inorg. Biochem.*, 1993, **52**, 17.
31 W. Bal, M. Jeżowska-Bojczuk and K. S. Kasprzak, *Chem. Res. Toxicol.*, 1997, **10**, 906.
32 P Młynarz, W. Bal, T. Kowalik-Jankowska, M. Stasiak, M. T. Leplawy and H. Kozłowski, *J. Chem. Soc.*, *Dalton Trans.*, 1999, 109.
33 K. Varnagy, J. Szabo, I. Sovago, G. Malandrinos, N. Hadjiliadis, D. Sanna and G. Micera, *J. Chem. Soc.*, *Dalton Trans.*, 2000, 467.
34 L. D. Pettit, S. Pyburn, W. Bal, H. Kozłowski and M. Bataille, *J. Chem. Soc.*, *Dalton Trans.*, 1990, 3565.
35 G. F. Bryce, R. W. Roeske and F. R. N. Gurd, *J. Biol. Chem.*, 1966, **241**, 1072.
36 B. Decock Le Reverend, F. Liman, C. Livera, L. D. Pettit, S. Pyburn and H. Kozłowski, *J. Chem. Soc.*, *Dalton Trans.*, 1988, 887.
37 M. A. Zoroddu, T. Kowalik-Jankowska, H. Kozłowski, H. Molinari, K. Salnikow, L. Broday and M. Costa, *Biochim. Biophys. Acta*, 2000, **1475**, 163.
38 W. Bal, M. Dyba and H. Kozłowski, *Acta Biochim. Pol.*, 1997, **44**, 467.
39 W. Bal, M. Dyba, F. Kasprzykowski, H. Kozłowski, R. Latajka, L. Łankiewicz, Z. Mackiewicz and L. D. Pettit, *Inorg. Chim. Acta*, 1998, **283**, 1.
40 P. Młynarz, N. Gaggelli, J. Panek, M. Stasiak, G. Valensin, T. Kowalik-Jankowska, M. T. Leplawy, Z. Latajka and H. Kozłowski, *J. Chem. Soc.*, *Dalton Trans.*, 2000, 1033.
41 H. Kozłowski, W. Bal, M. Dyba and T. Kowalik-Jankowska, *Coord. Chem. Rev.*, 1999, **184**, 319.
42 W. Bal, M. Jeżowska-Bojczuk, H. Kozłowski, L. Chruściński, G. Kupryszewski and B. Witczuk, *J. Inorg. Biochem.*, 1995, **57**, 235.
43 G. F. Bryce, R. W. Roeske and F. R. N. Gurd, *J. Biol. Chem.*, 1965, **240**, 3837.
44 G. F. Bryce and F. R. N. Gurd, *J. Biol. Chem.*, 1966, **241**, 122.
45 T. G. Fawcett, E. E. Bernarducci, K. Krogh-Jespersen and H. J. Schugar, *J. Am. Chem. Soc.*, 1980, **102**, 2598.
46 B. Gyurcsik, I. Vosekalna and E. Larsen, *Acta Chem. Scand.*, 1997, **51**, 49.
47 M. A. Zoroddu, T. Kowalik-Jankowska, H. Kozłowski, K. Salnikow and M. Costa, *J. Inorg. Biochem.*, in press.
48 L. D. Pettit, J. E. Gregor and H. Kozłowski, in *Perspectives on Bioinorganic Chemistry*, eds. R. W. Hay, J. R. Dilworth and K. B. Nolan, JAI Press, London, 1991, vol. 1, p. 1.
49 B. Barszcz, J. Kulig, J. Jezierska and J. Lisowski, *Pol. J. Chem.*, 1999, **73**, 447.
50 J. H. Viles, F. E. Cohen, S. B. Prusiner, D. B. Goodin, P. E. Wright and H. J. Dyson, *Proc. Natl. Acad. Sci. USA*, 1999, **96**, 2042.
51 C. Vita, Ch. Roumestand, F. Toma and A. Menez, *Proc. Natl. Acad. Sci. USA*, 1995, **92**, 6404.